A Highly Effective and Efficient Cost-Function-Reduction Method for Inverse Lithography Technique

Jinyu Zhang, Wei Xiong, Yan Wang, and Zhiping Yu
Institute of Microelectronics
Tsinghua University
Beijing, China, 100084
E-mail address: zhangjinyu@tsinghua.edu.cn

Min-Chun Tsai
Advanced Technology Group
Synopsys Inc.
Mountain View, CA, 94043, USA
E-mail address: Min-Chun.Tsai@synopsys.com

Abstract—**An efficient algorithm based on the pixel-based mask representation is proposed for fast synthesis of model-based inverse lithography technology (ILT) to improve the resolution and pattern fidelity in optical lithography. This new algorithm uses perturbation method to reduce N^2 intensity computations to only three (3) equivalent intensity computations, where N^2 is the total number of pixels in a mask. This algorithm has been demonstrated using different critical dimensions (CDs) and different mask technologies with incoherence and partial-coherence image systems. Good fidelity images are achieved when CD is reduced to 45nm.**

Keywords- ILT; CFRM; partial-coherence image system

I. INTRODUCTION

Resolution Enhancement Technologies (RETs) are widely used to cope with the severe optical distortions in sub-wavelength lithography. It is a big challenge, however, in resolving finer patterns of 32nm or 22nm technique node.

Pixelization based Inverse Lithography Technique (ILT) has been proposed [1][2] as an option for RET. The pioneer work in ILT was by Saleh et al. [1]. Sherif [2] employed iterative-alternating-projections approach to synthesize binary masks. Liu and Zakhor [3] used simulated annealing (SA) and Pati and Kailath [4] used POCS (Projection on Convex Sets), respectively, to synthesize phase shift masks. Oh [5] used random-pixel flipping, and Erdmann [6] proposed genetic algorithms (GA) to solve the above problem. Granik [7] used nonlinear programming to solve the inverse problem. Pang [8] used level-set method to do optimization. Recently, Borodovsky[9] proposed RET-Pixelated Phase Mask (PPM) as a novel lithography RET. Poonawala and Milanfar [10] [11] developed a gradient-based method to perform optimization. The gradient-based method, however, only focused on incoherence and coherence image systems. David and Bollepalli [12] have described ILT suitable to partial-coherence image system.

ILT is an ill-posed problem. Its convergence depends strongly on initial conditions and optimization schemes. Technology-scaling aggravates the convergence issue further due to reduced ratio of pattern to pixel sizes (PP-ratio). The reduced PP-ratio comes from mask-making technology cannot keep up with technology-scaling. In this paper, we developed an effective and efficient ILT algorithm to mitigate those issues. This new Cost-Function-Reduction method (CFRM) reduces N^2 intensity computations to three (3) equivalent intensity computations. This algorithm has been demonstrated using different critical dimensions (CDs) and mask technologies. Good fidelity images have been achieved when CD is reduced to 45nm with 15×15 nm^2 pixel size.

II. PHYSICAL MODEL

The physical model and image system have been discussed in our previous work [14]. We applied this algorithm to five different mask technologies, i.e. binary, APSM, 6%EPSM, 18%EPSM and, strong PSM respectively. Masks are first discretized to pixels and each pixel is initialized with specified amplitude transmission coefficient. Table 1 shows transmission coefficients for various mask technologies.

Table 1. Transmission coefficients for various mask technologies, where minus sign means that the transmitted light has a phase shift of 180°.

Mask technologies	Allowable transmission coefficient
Binary	0 or +1
6%EPSM	-0.245 or +1
18%EPSM	-0.4243 or +1
APSM	-1 or 0 or +1
Strong PSM	-1 or +1

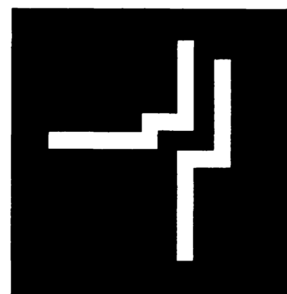

Fig. 1 The desired "double snake" pattern on wafer.

To demonstrate our algorithm, we used a "double snake" pattern (shown in Fig. 1), which is a typical "difficult" layout of Metal 1 (M1) pattern. The pixel size and mask size are CD related. When CD equals 100nm and 75 nm, the pixel size is $25\times25\text{nm}^2$. For smaller CDs, namely 60nm and 45nm, the pixel size is $15\times15\ \text{nm}^2$. Mask sizes range from 48×48 to 64×64.

III. METHODOLOGY

In the CFRM algorithm, ILT is solved through iterations. In each iteration, two steps are performed. First we calculate the cost function reduction with respect to pixel-flipping on the whole mask. Then the most effective pixel is flipped to reduce the cost function. In the past, the first step required N^2 intensity calculations on an $N\times N$ pixel mask, which made the calculation computationally intractable, such that people were forced to use alternative methods and depended strongly on the initial condition. In this work, we developed a new method that reduces the required N^2 calculations to merely 3 calculations and thus provides an effective reduction and highly efficient computation.

We treat each pixel as an independent variable and use perturbation method to approximate the cost function change by all pixels flipped on the mask. To calculate cost function derivatives, the sigmoid function is used to approximate the resist effect,

$$\text{sig}(u) = \frac{1}{1+e^{-b(u-u_r)}} \tag{1}$$

, where parameter b dictates the steepness of the sigmoid and is set to a large number in our calculation. The parameter u_r is the threshold parameter of the sigmoid and is set to the threshold level of the resist.

The cost function can be defined as follows

$$E_C = \sum_{i,j=1}^{N} \left\{\text{sig}[I(i,j)] - z(i,j)\right\}^2 \tag{2}$$

, in which E_C is the cost function, (i, j) is the pixel position on mask and sig[•] is the sigma function which approximates the resist effect. $z(i,j)$ is the desired mask pattern and $I(i,j)$ is the optical intensity at pixel (i,j).

A. Calculate the Cost Function Change

The cost-function-reduction is defined by change of E_C, i.e., ΔE_C, with respect to the change of mask-transmission, Δm. ΔE_C is an $N\times N$ matrix and requires N^2 intensity computations which makes the computation infeasible. To solve this issue, we first approximate ΔE_C by the Taylor series as follows

$$\Delta E_C \approx \frac{\partial E_C}{\partial m} \circ \Delta m + \frac{1}{2}\frac{\partial^2 E_C}{\partial m^2} \circ \Delta m^2 \tag{3}$$

, where $\circ$ denotes element-by-element multiplication operator. m and Δm are current mask-transmission and mask-transmission change matrix. And then for incoherence image systems, the 1st and 2nd derivatives of E_C in Eq. (3) can be derived as

$$\frac{\partial E_C}{\partial m} = -2h \otimes \left\{(z - sig(I)) \circ sig'(I)\right\}$$
$$\frac{\partial^2 E_C}{\partial m^2} = -2(h \circ h) \otimes \left\{(z - sig(I)) \circ sig''(I) - sig'(I) \circ sig'(I)\right\} \tag{4}$$

, where h is impulse response function in incoherence image system and $\otimes$ denotes convolution. Eq. (4) reduces the ΔE_C calculation to three intensity-equivalent computations, one for I, the other two for 1st and 2nd derivatives of E_C, respectively.

For a partial-coherence image system, one intensity computation includes several convolution operations. The intensity $I(i,j)$ is defined as follows

$$I(i,j) = \sum_{l=1}^{K} \lambda_l \left|[m \otimes h_l](i,j)\right|^2 \tag{5}$$

, where complex matrix h_l for l=1,2,…,K is for the amplitude spread functions (also referred to as optical system kernels) of the coherent systems. λ_l are the singular values and decrease rapidly as l increases. K is the number of expansion terms. Similarly, the 1st and the 2nd derivatives of E_C can be derived.

In practice, higher order derivatives of E_C can be used in Eq. (2) if needed. From our experiments, it was found that 2nd order derivative is sufficient for ΔE_C approximations with average relative error of 0.7%, as shown in Fig. 2(a). Fig. 2(b) compares ΔE_C profile among 1st derivative, 2nd derivative approximation and exact solutions along the cut line in Fig. 1(a).

Note that various mask technologies can be easily implemented with the aid of Δm and the pixel values maintain discrete during optimization. The mask-transmission change matrix Δm in Eq. (3) is determined by mask technologies and current pixel values. Here we use binary mask as an example to illustrate how to determine Δm for a specific mask technology. For a binary mask, if a pixel current value is 0, since flipping the pixel means the value of the pixel should be changed from 0 to 1, the change of the pixel equals 1. Similarly, when a pixel current value is 1, the change of the pixel equals -1. So matrix elements of Δm for binary mask consist of -1 or 1. Table 2 shows a pixel value change for a given mask technology and its current pixel value. By modifying the corresponding Δm matrix, different mask technology can be implemented easily. Also, the pixel value can be kept discrete throughout the optimization.

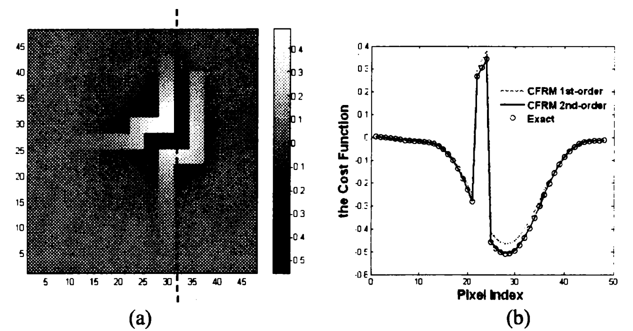

(a) (b)

Fig. 2 (a) 2D plot of ΔE_c and (b) 1D profile of ΔE_c along the cut line of the mask calculated by different methods. CD equals 45nm and pixel size is $15\times15\text{nm}^2$.

Table 2. A pixel value change Δp for various mask technologies. Δp is related to its current pixel value p and mask technologies.

Mask technologies	p	Δp	p	Δp	p	Δp
Binary	+1	-1	0	1	-	-
6%EPSM	+1	-1.245	-0.245	1.245	-	-
18%EPSM	+1	-1.424	-0.424	1.424	-	-
APSM	+1	-1, -2	0	1,-1	-1	1,2
Strong PSM	+1	-2	-1	2	-	-

B. Pixel Flipping

In the second step of each iteration, the most effective pixels, namely the pixel corresponding to larger negative value in ΔE_C, is selected to flip. After flipping pixels, the mask has been updated. This process is repeated to calculate ΔE_C for a new mask and then pixels are selected to flip until the most negative matrix element of ΔE_C becomes smaller (less negative) than a preset termination criterion ε.

Note that the fidelity of the final wafer pattern is closely related to ε. If ε is smaller, more pixels may have to be flipped to reduce the cost function and the image fidelity will increase. Generally speaking, pixels with more negative value are around the original desired pattern in ΔE_C. More negative ε then will lead less complex mask pattern but less fidelity of final image. More assisted features (AFs) are created automatically to improve the image fidelity when smaller ε is used.

IV. RESULTS AND DISCUSSION

Fig. 3(a) shows the desired pattern and output pattern without RET with an incoherence image system. The pixel size equals 25nm×25nm. The convergence process is shown in Fig. 3(b) to demonstrate that the ILT algorithm works effectively.

Fig. 4 show the synthesis mask patterns using different initial conditions. The initial patterns are full zeros, full ones and the desired pattern, shown in for Fig. 4(a), (b) and (c), respectively. The fidelity of the patterns on wafer is almost the same for the three cases. Fig. 4(d) shows the comparison result between the final pattern on wafer and the desired one. Good fidelity of the image on wafer is achieved. The final synthesis mask patterns with quite different initial conditions are quite similar. These results indicate that CFRM is quite robust. We speculate that the final results may approach to the global minimum. Note that the different initial conditions will have a significant influence on the convergence rate.

Fig. 3(a) shows the desired pattern and output pattern without RET with a partial coherence image system. Note that when CD equals to 45nm and 60nm, there is 'nothing' on wafer. The convergence process is shown in Fig. 3(b) for CD = 45nm and binary mask optimization.

Fig. 6-8 show ILT results for different CDs and mask technologies. In these figures, the left graph is the final synthesis mask and the right one is comparison between final image on wafer and desired pattern, respectively. All these results are calculated using the partial-coherence image system. Initial mask is the desired pattern althought it produces 'nothing' when CD=45nm and 60nm. It can be seen that good fidelity is achieved in very small CDs and CDs are only 3 or 4 times of pixel sizes. Since ΔE_C can be calculated efficiently and accurately, our ILT algorithm can find every pixel that reduces ΔE_C regardless of the initial pattern. The most effective pixel is then flipped to reduce ΔE_C.

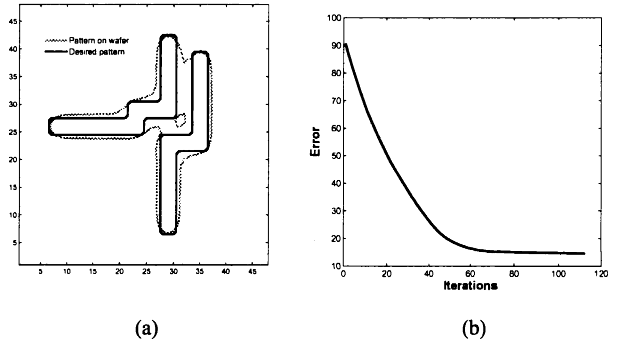

Fig. 3 (a) The desired pattern and output wafer pattern without RET for the incoherence image system when CD = 75nm, pixel size equals 25nm× 25nm. (b) Convergence process for CD=75nm optimization.

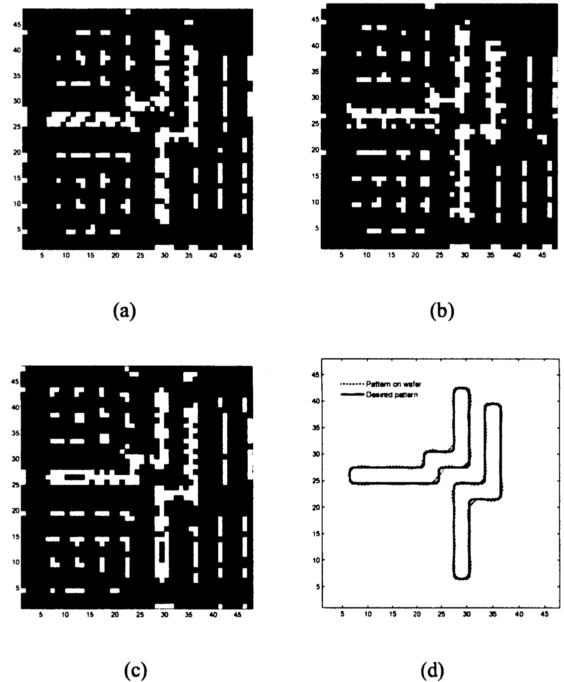

Fig. 4 The synethesis mask patterns with different initial conditions. The initial mask patterns for (a), (b) and (c) are full zeros, full ones and the desired pattern, respectively. White and black pixels have a pixel value of 1 and 0, respectively. (d) is comoparison between the final pattern on wafer and the desired pattern, where CD=75nm, incoherence image system, pixel size equals 25nm×25nm.

V. SUMMARY

We have derived an effective and efficent ILT algorithm to handle small CD mask patterns. The algorithm is based on CFRM which reduces N^2 intensity computations to 3 intensity-equivalent computations. Various mask technologies can be easily implemented. Good fidelity of image is achieved when CD is reduced to 45nm.

ACKNOWLEDGMENT

This work is funded by Basic Research Foundation of Tsinghua National Laboratory for Information Science and Technology (TNList).

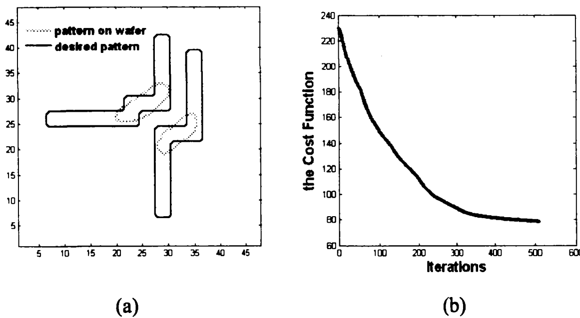

Fig. 5 (a) The desired pattern and output wafer pattern without RET for the partial-coherence image system when CD = 75nm. There is 'nothing' when CD equals 45 and 60nm. (b) Convergence process for CD=45nm optimization.

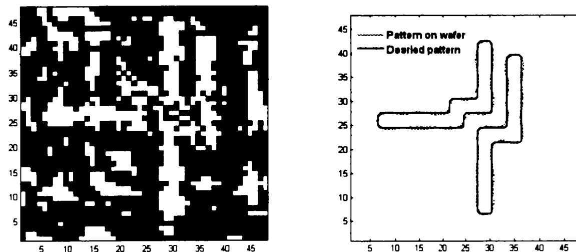

Fig. 6 ILT optimization results when CD = 75nm. The mask type is binary. Black and white pixels have a pixel value of 1, 0 respectively. Pixel size is $25\times25nm^2$.

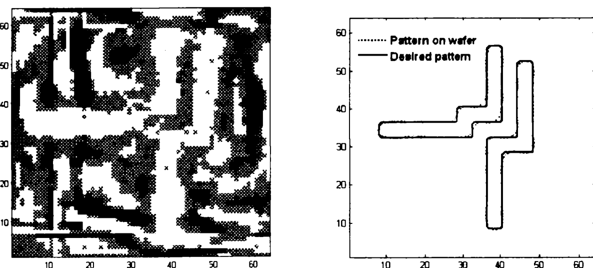

Fig. 7 ILT optimization results when CD = 60nm. The mask type is APSM. White, grey and black pixels have a pixel value of 1, 0, and -1, respectively. Pixel size is $15\times15nm^2$.

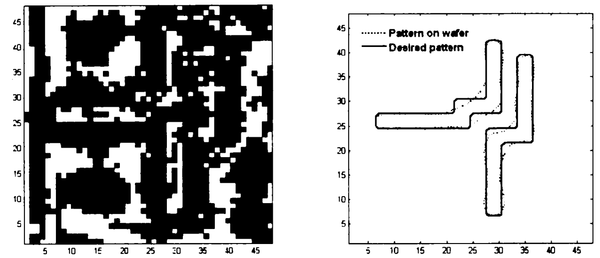

Fig. 8 ILT optimization results when CD = 45nm, The mask type is strong PSM. White and black pixels have a pixel value of 1 and -1, respectively. Pixel size is $15\times15nm^2$.

REFERENCES

[1] B.E.A Saleh and S. I. Sayegh, "Reduction of errors of microphotographic reproductions by optimal corrections of original masks", Opt. Eng. 20, 781-787(1981).

[2] S. Sayegh and B. Saleh, Image design: Generation of a prescribed image at the output of a bandlimited system, IEEE Transcation on Pattern Analysis and Machine Intelligence 5, 441−445 (1983).

[3] Sherif Sherif and Bahaa Saleh, "Binary Image Synthesis Using Mixed Linear Integer Programming", IEEE Trans. Image Processing, 4, 1252-1257(1995).

[4] Y. Liu and A. Zakhor, "Binary and phase shifting mask design for optical lithography," IEEE Transactionson Semiconductor Manufacturing 5, 138–151(1992).

[5] V. Pati and T. Kailath, "Phase-shifting masks for microlithography: Automated design and mask requirements," Journal of Optical Society of America A - Optics Image Science and Vision 9, 2438–2452 (1994).

[6] Y. Oh, J. C. Lee, and S. Lim, "Resolution enhancement through optical proximity correction and stepper parameter optimization for 0.12-μ m mask pattern", Proc. SPIE 3679, 607–613(1999).

[7] A. Erdmann, R. Farkas, T. Fuhner, B. Tollkuhn, and G. Kokai, "Towards automatic mask and source optimization for optical lithography", Proc. SPIE 5377, 646–657(2004).

[8] Y. Granik, "Solving inverse problems of optical microlithography", Proc. SPIE 5754, 506–526 (2005).

[9] L. Pang, Y. Liu , D. Abrams, "Inverse Lithography Technology (ILT) for Advanced Semiconductor Manufacturing", J. Exp. Mech. 22, 295(2007).

[10] Y. Borodovsky, W. Cheng, R. Schenker, V. Singh, "Pixelated Phase Mask as Novel Lithography RET", Proc. SPIE 6924, 69240E(2008).

[11] A. Poonawala and P. Milanfar, "OPC and PSM design using inverse lithography: A non-linear optimization approach", Proc. SPIE 6154, 61543H1–61543H14(2006).

[12] A. Poonawala and P. Milanfar, "Fast and low-complexity mask design in optical microlithography - an inverse imaging problem", IEEE Trans. on Image Proc. 16 (2007).

[13] Paul S. Davids and Srinivas B. Bollepalli, "Generalized Inverse Problem for Partially Coherent Projection Lithography", Proc. SPIE 6924, 69240X(2008).

[14] J. Zhang, W. Xiong, M. Tsai, Y. Wang and Z. Yu, "Efficient Mask Design for Inverse Lithograph Technology Based on 2D Discrete Cosine Transformation (DCT)", SISPAD, 49-52, 2007.